

## MORPHOLOGY OF PRE-NOON AND POST-NOON AURORAS

Masaru AYUKAWA<sup>1</sup>, Kazuo MAKITA<sup>2</sup>, Masanori NISHINO<sup>3</sup>,  
Pat NEWELL<sup>4</sup> and Ching-I. MENG<sup>4</sup>

<sup>1</sup>*National Institute of Polar Research, Kaga 1-chome, Itabashi-ku, Tokyo 173-8515*

<sup>2</sup>*Takushoku University, 1-815, Tatemachi, Hachioji-shi, Tokyo 193-0944*

<sup>3</sup>*STE Lab., Nagoya University, Honohara, Toyokawa 442-8507*

<sup>4</sup>*APL, The Johns Hopkins University, 11100 Johns Hopkins Road,  
Laurel, MD 20723-6099, U.S.A.*

**Abstract:** General characteristics of dayside auroras for quiet and disturbed conditions are examined on the basis of Greenland and Spitzbergen TV data. It is our new finding that characteristics of dayside auroras are quite different between the pre- and post-noon sectors. Namely, corona auroras are seen in the pre-noon sector and band auroras are seen in the post-noon sector. During the quiet period, corona auroras are observed at magnetic latitudes higher than  $75^\circ$  in the pre-noon sector. In the post-noon sector, no remarkable auroras are seen around  $75^\circ$  MLAT. On the other hand, during the disturbed period, corona auroras are observed at latitudes lower than  $80^\circ$  MLAT in the pre-noon sector. Periodic bright band auroras appear in the post-noon sector. The comparison between these auroras and particle precipitation is also examined and the source region of dayside auroras is discussed.

### 1. Introduction

The study of dayside aurora and its related phenomena gives us essential information to understand the interaction process between solar wind and the dayside magnetopause. The characteristics of dayside auroras were examined by many researchers with the ground and satellite observations (VOROBYEV *et al.*, 1975; SANDHOLT *et al.*, 1983; EGELAND *et al.*, 1992; ELPHINSTONE *et al.*, 1992; SMITH, 1994; MENG, 1994; AYUKAWA *et al.*, 1997).

From the Viking satellite observation of ultraviolet imager, ELPHINSTONE *et al.* (1993) summarized the dayside auroral morphologies. They examined FTE-like auroral forms and impulsive low latitude forms in the post-noon sector. A new auroral display termed "impulsive low latitude auroral form" occurs in association with ground magnetic pulsation (a period of about 3 min). An impulse in the solar wind density appears to be directly related to the onset of this aurora. This may indicate an excitation of MHD waves inside the magnetosphere.

On the basis of ground auroral observations, several remarkable results have been reported by a number of researchers. Among them, SANDHOLT *et al.* (1989) examined the dayside aurora at Ny-Ålesund and showed a sudden poleward movement of dayside aurora. They called this phenomenon as "dayside auroral break up". FASEL *et al.* (1994) also examined poleward-moving auroral forms (PMAFs). They defined PMAFs as rayed arcs or bands that are formed in the dayside auroral oval and drift into the polar cap. These auroral phenomena show a dependence on the interplanetary magnetic field (IMF) which make them as candidates for the ionospheric signatures of flux

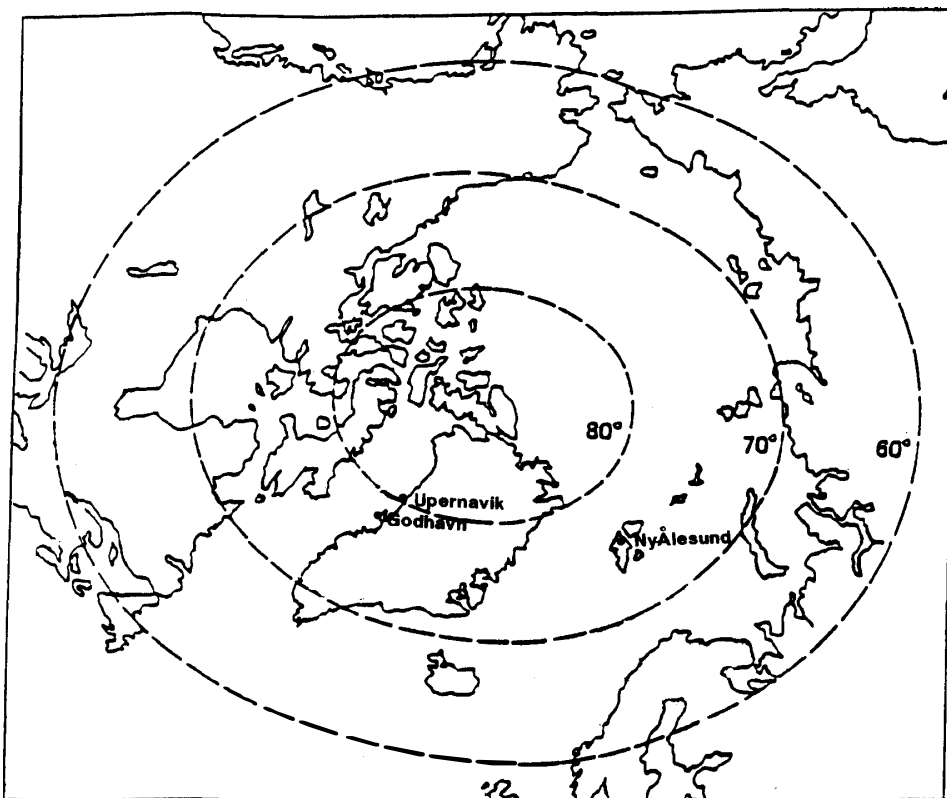


Fig. 1. The location of Godhavn ( $76.6^\circ$  MLAT), Upernavik ( $80.2^\circ$  MLAT) and Ny-Ålesund ( $75.9^\circ$  MLAT) in geomagnetic coordinate. The time difference between magnetic local time (MLT) and universal time (UT) is  $MLT = UT - 2$  hours at Greenland stations and  $MLT = UT + 3$  hours at Ny-Ålesund.

transfer events (SOUTHWOOD, 1987). Although many researchers examined dayside auroral phenomena and obtained various results, characteristics of dayside auroras are not sufficiently understood yet. This is because the ground-based observation is limited to the winter dark conditions and furthermore, there are few auroral observatories at high enough latitude to observe the noon sector aurora.

In order to make clear the characteristics of dayside auroral phenomena, we carried out auroral observations at high latitude regions during Solar-Terrestrial Energy Program (STEP) period. It was newly found that different types of aurora are seen in the pre- and post-noon sectors from all-sky TV data. Figure 1 shows the location of all-sky TV observations at Godhavn ( $76.6^\circ$  MLAT), Upernavik ( $80.2^\circ$  MLAT) in Greenland and Ny-Ålesund ( $75.9^\circ$  MLAT) in Spitzbergen. Since the geographic latitudes of Greenland stations are not so high, the observable period for dayside auroras is limited and auroral phenomena in the pre-noon sector can be detected at Godhavn and Upernavik. The magnetic local time (MLT) at these Greenland stations is behind from the universal time (UT) by 2 hours ( $MLT = UT - 2$  hours) and it is advanced from universal time by 3 hours ( $MLT = UT + 3$  hours) at Ny-Ålesund. The difference between Greenland and Spitzbergen in magnetic local time is about 5 hours, so the pre-noon and post-noon auroral phenomena can be examined by comparing these two regions simultaneously.

We selected and examined two typical dayside auroral phenomena during the quiet

period (January 10, 1994) and the disturbed period (January 12, 1994). We also compared the simultaneous particle data obtained by DMSP satellite. During these periods, three DMSP satellites (F8, F10, F11) passed over the polar region. Among them, DMSP/F8 satellite was in the noon-midnight orbit but mainly passed through only in the night side sector. DMSP/F 11 satellite also passed over in the noon-midnight sectors but there were many data gaps. Therefore, we examined mainly DMSP/F 11 orbit data in this paper.

## 2. Dayside Aurora and Simultaneous Particle Precipitation during Quiet Period

The typical auroral phenomena during quiet period (09h to 12h UT January 10, 1994) are examined by using auroral TV data at Greenland and Spitzbergen. Figure 2 shows the geomagnetic data plots (Kyoto University, 1994). Although these plots are provisional and it does not contain enough worldwide geomagnetic station's data, geomagnetic activities at the high and low latitude regions seem to be quiet and the  $K_p$  index is continuously 0 or 1 during this period. The interplanetary magnetic field data (IMF) observed by the IMP 8 satellite is shown in Fig. 3. During the period from 09–12h UT, the intensity of IMF  $|B| = 8\text{--}9$  nT,  $B_x = 0\text{--} -5$ ,  $B_y = -3\text{--} +8$  and  $B_z = -2\text{--} +7$  nT, respectively. It is noted that the  $B_z$  component is almost positive during this interval except the impulsive negative value at about 1020 UT.

The auroral data at two stations in Greenland is illustrated in Fig. 4. The auroral dynamic spectrum along the north-south meridian are examined from the all-sky TV data obtained at the two stations. The upper and lower spectra show the auroral movement and the intensity at Upernavik and Godhavn stations, respectively. The corona type auroras are frequently observed at Upernavik during the interval from 08h to 10h UT. A certain corona aurora shift from the equatorward to the poleward and after then, another corona aurora appears and moves to the poleward quasi periodically. The appearances period of these corona is 300–400 s. The auroral activity becomes low during 1000 to 1030 and after then corona auroras are frequently observed again at Upernavik. It is noted that active corona auroras appear at magnetic latitudes higher than  $75^\circ$  MLAT during the quiet period.

On the other hand, arc or band auroras propagate from the dayside region towards the zenith of Godhavn during the period from 0800 to 0920 UT. The corona auroras move further from the zenith to the poleward side of Godhavn after 0920 UT. In this case, it is difficult to observe auroral phenomena near the noon meridian at Godhavn because the sunlight disturbs the auroral observation. However, corona auroras are observed near the noon meridian ( $\sim 10$ h MLT) at Upernavik. Although we have not examined the local time dependence of the occurrence frequency of corona aurora yet, the activity of corona aurora generally becomes stronger as the station reaches nearer to the noon meridian.

All-sky TV data at Upernavik and Godhavn during above quiet period (Fig. 4) are illustrated in Fig. 5. Upper and lower all-sky data are obtained at Upernavik and Godhavn, respectively. In the upper left data at 0919:19 UT, corona auroras are observed near the zenith and also on the equatorward side. These corona auroras

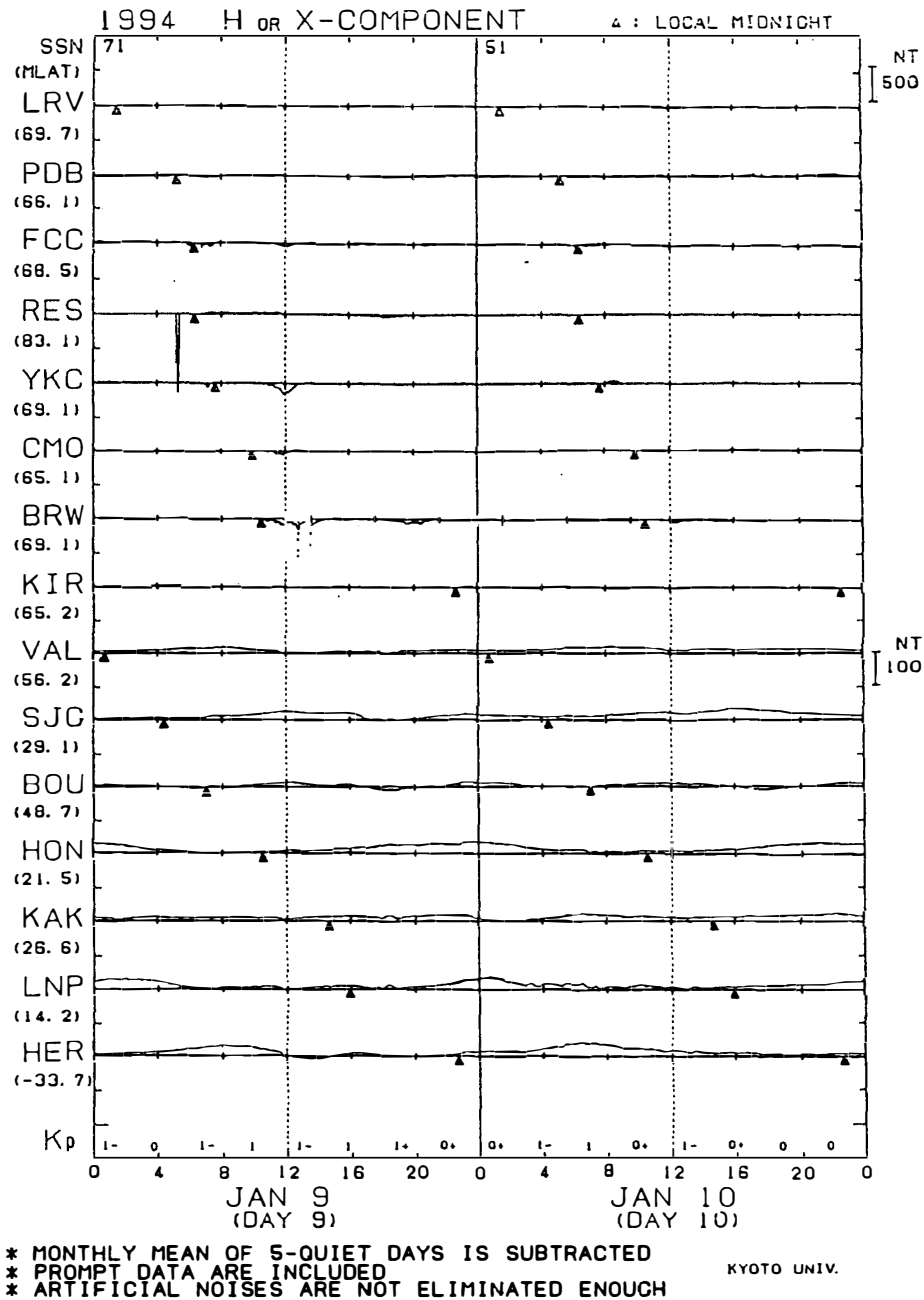


Fig. 2. The provisional geomagnetic data plots. The worldwide geomagnetic activity is very low during the interval from 09h to 12h UT on January 10. Kp index in this period is 0+.

generally move poleward quasi-periodically. Namely when corona disappears in the poleward region, another corona appears again and moves poleward. In the lower left data at 0919:26 UT, a band aurora is seen near the zenith of Godhavn and a corona aurora is seen on the poleward side. The luminosity of the poleward horizon is bright at Godhavn in this period, due to the reflection of town's lights from horizon's clouds. The band aurora develops from the east side (dayside) and propagates to the morning side. In the upper right data at 1040:03 UT, corona aurora is seen near the equatorward horizon. This corona corresponds to the bright corona near the zenith at Godhavn as shown in the lower right panel.

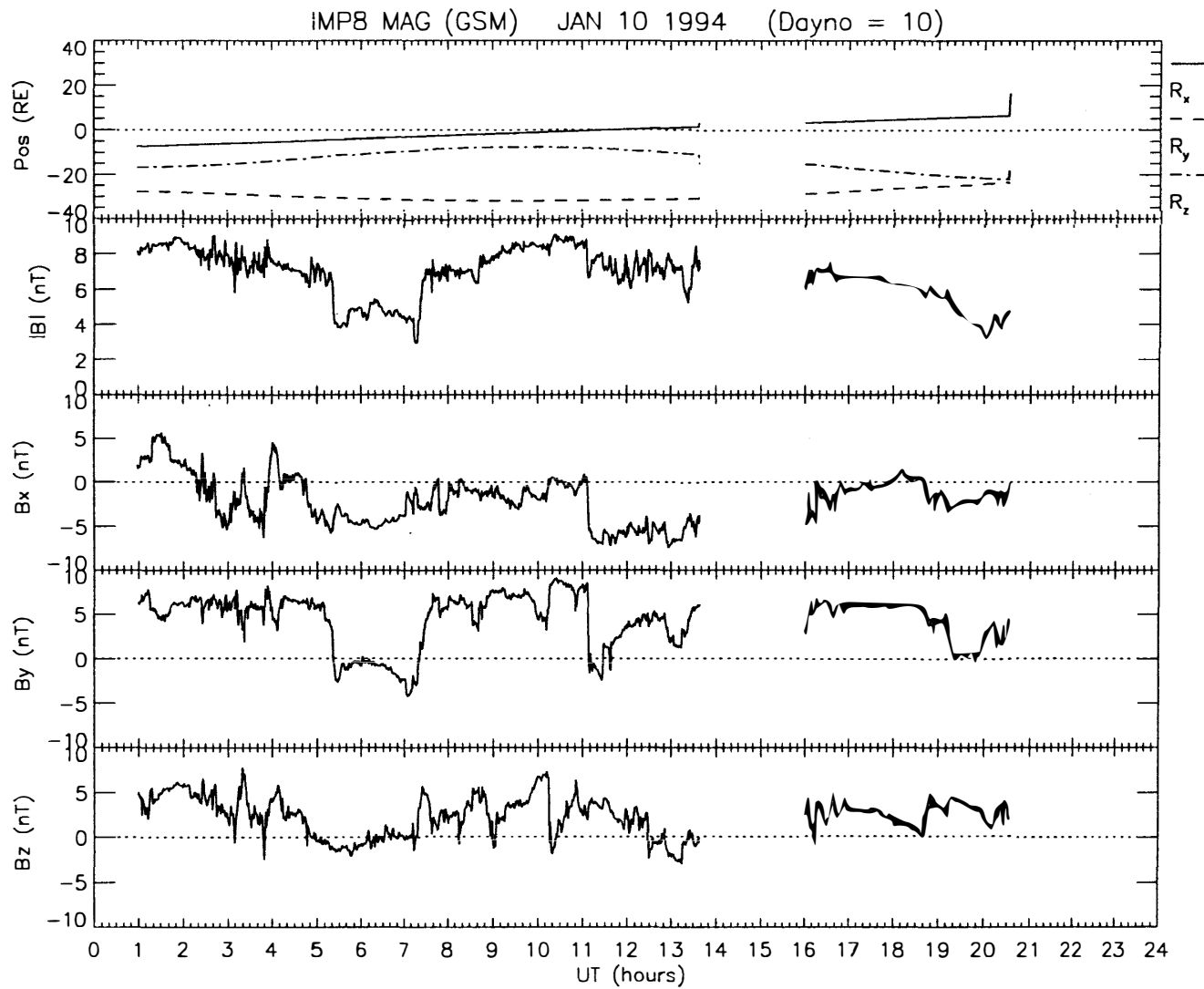


Fig. 3. Interplanetary Magnetic Field (IMF) data observed by IMP 8 satellite.

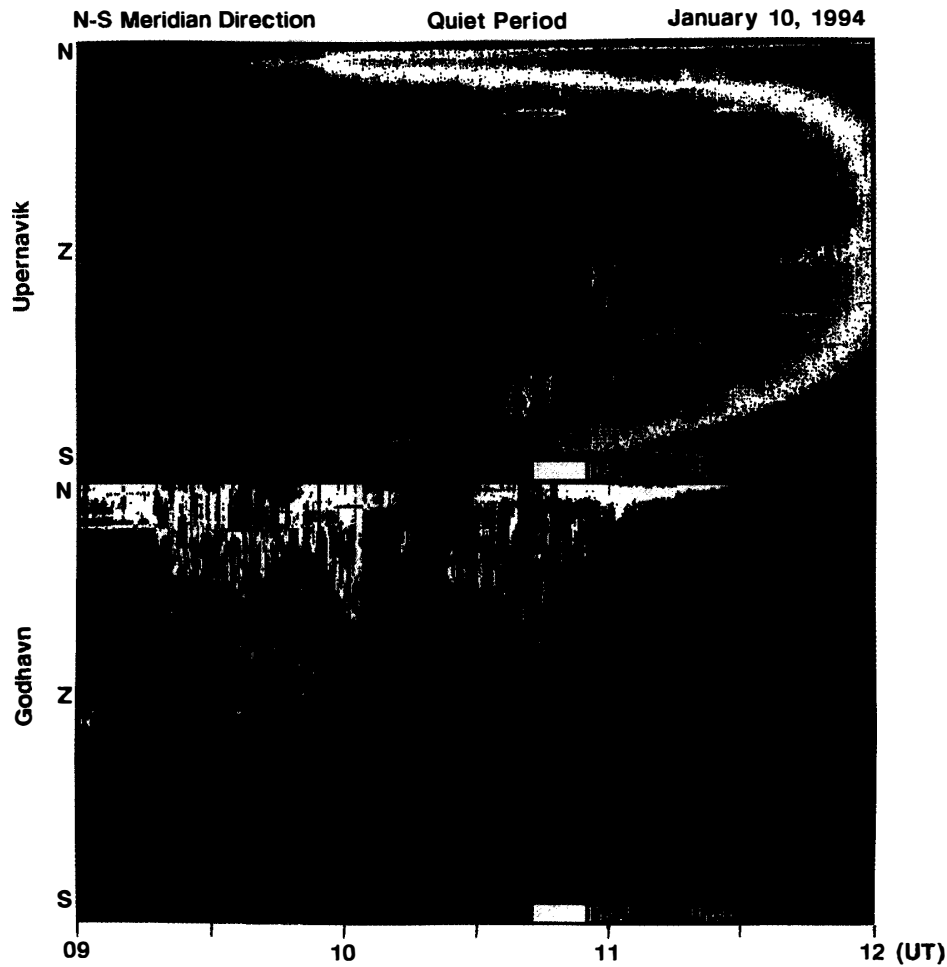


Fig. 4. The auroral dynamic spectra along the north-south meridian during quiet conditions. Upper and lower panels illustrate auroral spectra at Upernavik and Godhavn, respectively. Corona auroras are observed near the zenith of Upernavik and on the poleward side of Godhavn.

Figure 6 illustrates the auroral dynamic spectrum obtained at Ny-Ålesund during the period from 05 to 17h UT. Data format is the same as that of Fig. 4. Although faint auroras are observed during the period from 0815 to 0817 and 1320 to 1340 UT, the auroral activity is very low and no bright aurora is observed during this period. From the particle observation data as described later, the precipitation of electrons with energy less than 500 eV and ions with less than a few keV is observed on the poleward side of Ny-Ålesund during this quiet period. It suggests that the main precipitation region shifts poleward ( $>76^\circ$  MLAT) during the quiet condition.

In order to compare the particle precipitation with the ground auroral phenomena, the DMSP/F11 satellite particle data are examined for this quiet event. Figure 7 illustrates the DMSP satellite orbit and electron precipitation data obtained from 0830 to 1354 UT. The right panel's electron data (A, B, C, D) are obtained along satellite orbits (A, B, C, D) illustrated in the left panel. The electron data A was obtained during the interval from 0830 to 0847 UT. In this data, typical central plasma sheet (CPS) electrons are seen in the morning sector (0837–0840 UT). Impulsive low energy (less than 500 eV) precipitation are seen in the noon and post-noon sector at latitudes

### Quiet Period (January 10, 1994)

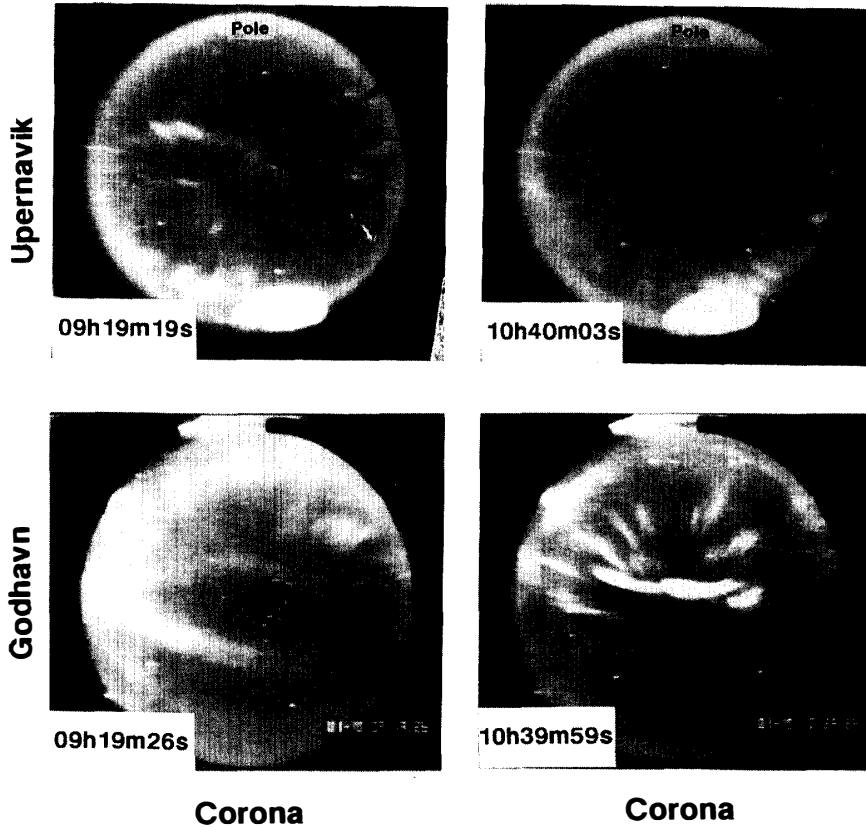


Fig. 5. All-sky TV camera data obtained at Upernavik and Godhavn. In the upper left panel, corona auroras are seen near the zenith of Upernavik in the early morning (0919:19 UT=0719:19 MLT). On the other hand when the station reaches near the noon sector, corona auroras appear on the lower latitude side and so they are observed near the zenith of Godhavn as shown in the lower right panel (1039:59 UT=0839:59 MLT).

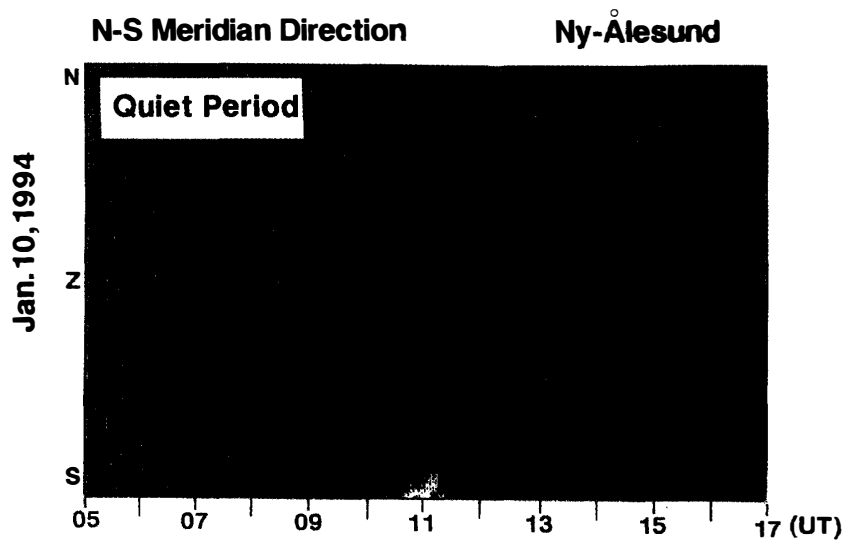


Fig. 6. The auroral dynamic spectrum obtained at Ny-Ålesund during the quiet condition from 05 to 17h UT on January 10, 1994. No remarkable bright auroras are observed during this interval.

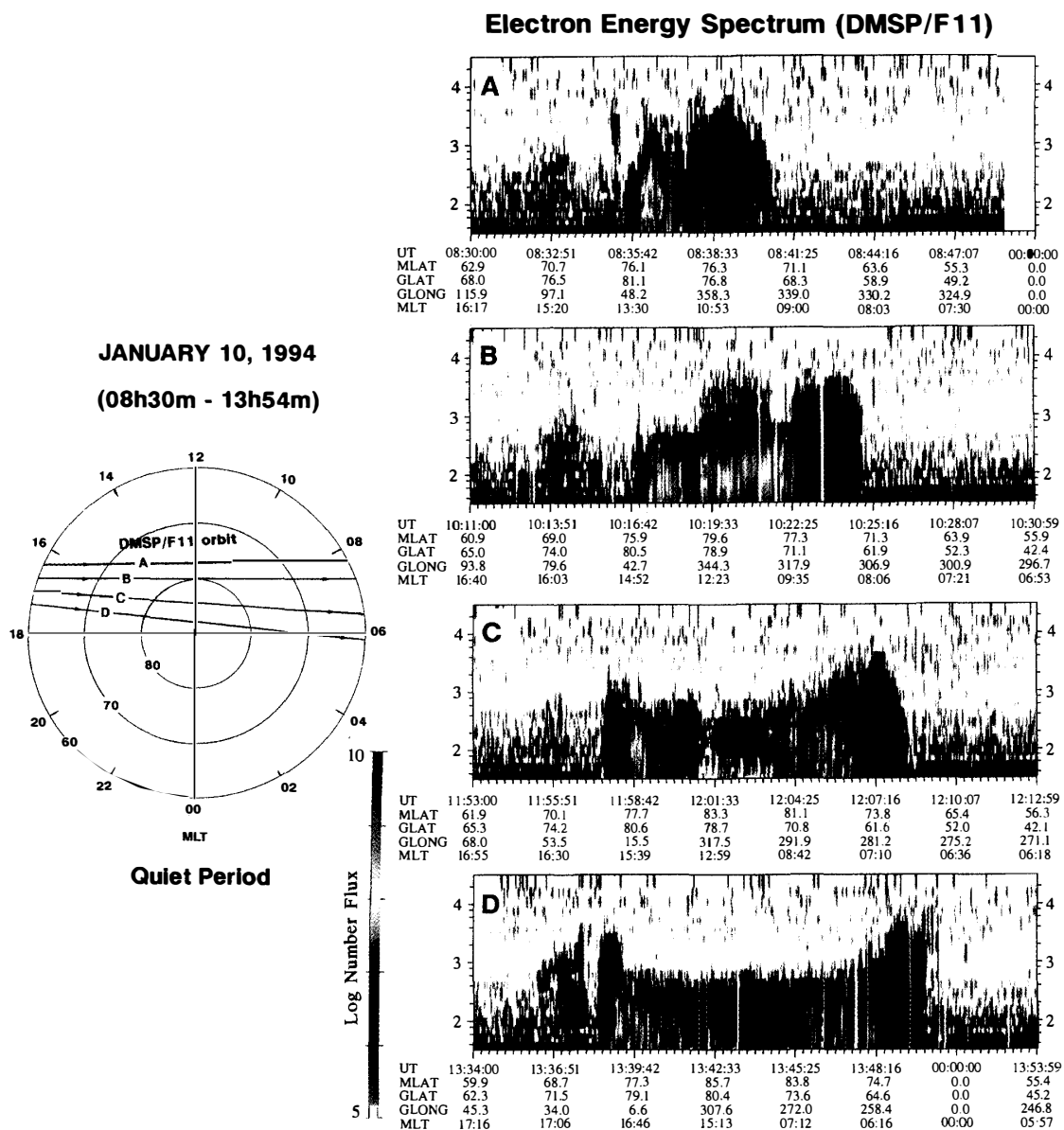


Fig. 7. DMSP/F11 satellite orbit and electron precipitation data during the quiet condition from 0830 to 1354 UT. The right panel electron data (A, B, C, D) are obtained along each satellite orbit A, B, C, D, respectively. It is noted that low energy electrons embedded all over the polar cap region.

higher than  $76^\circ$  MLAT (0835–0837 UT). The electron data B was observed during the per-iod from 1011 to 1031 UT. CPS electrons are also observed in the morning sector (1022–1025 UT) and low energy impulsive electrons are seen in the pre-noon and post-noon sector at latitudes higher than  $76^\circ$  MLAT (1016–1022 UT). The electron data C was observed during the period from 1153 to 1213 UT. It shows that CPS electrons are also observed at the equator side of the evening sector (1206–1208 UT) as well as in the morning sector ( $\sim 1158$ ). It is noted that impulsive low energy electron is seen in the morning (07–09h) at latitudes higher than  $80^\circ$  MLAT (1203–1207 UT). The electron data D was observed during the interval from 1334 to 1354 UT. Central plasma sheet precipitation is seen in both the evening ( $\sim 1339$  UT) and morning (1348–1350

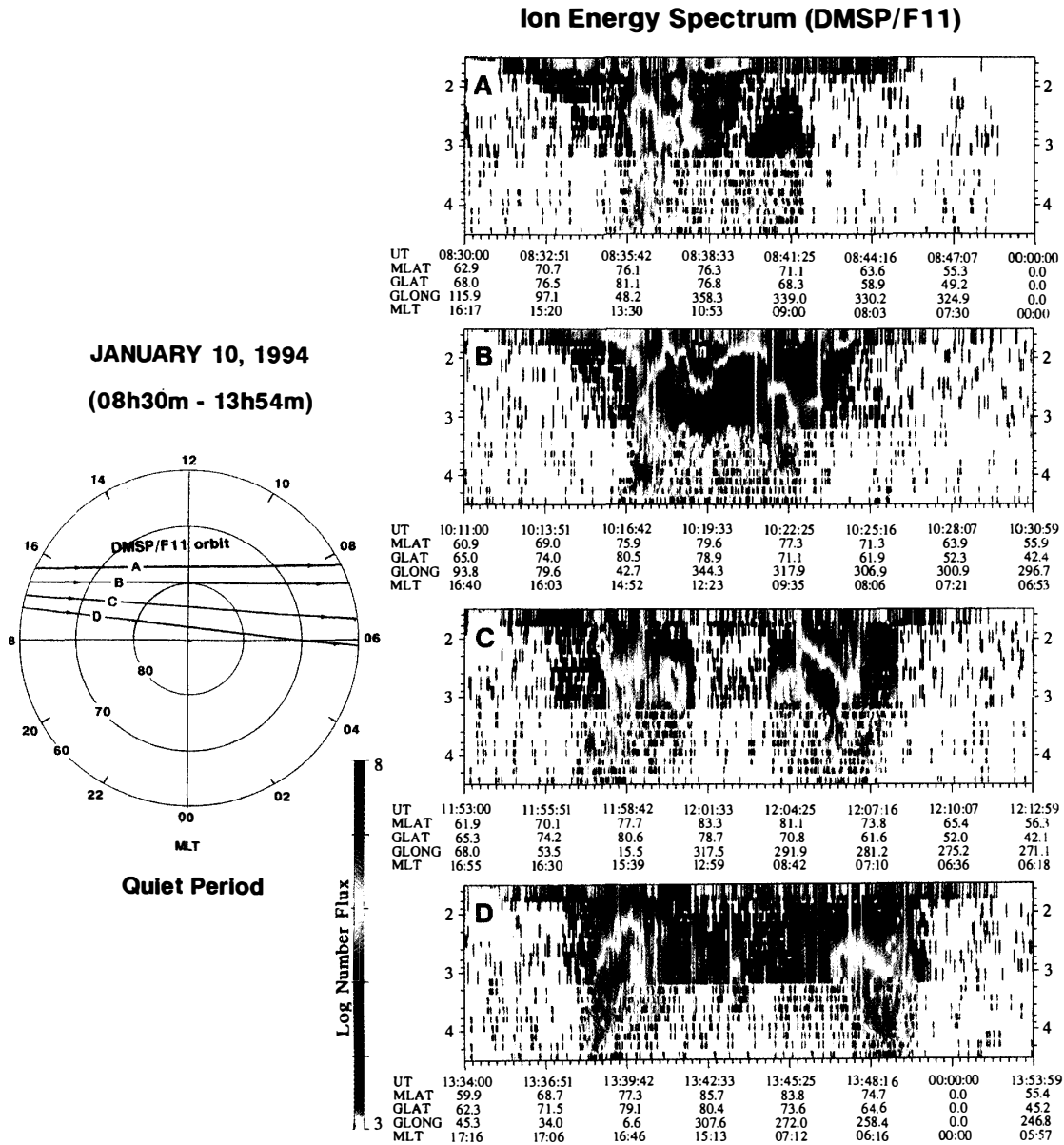


Fig. 8. DMSP/F11 satellite orbit and electron precipitation data during the quiet condition from 0830 to 1354 UT. The right panel ion data (A, B, C, D) are obtained along each satellite orbit A, B, C, D, respectively. It is noted that strong ion flux is observed in this period.

UT) sectors. In this orbit, the low energy impulsive electrons embed all over the polar region. This DMSP data suggest the possibility that the low energy electrons precipitating at higher latitude ( $>76$  degrees) excite auroral emission.

It is noted that the DMSP/F 11 satellite passed through the coverage of all-sky TV data at Upernavik (Orbit C) during the period from 1203:30 UT to 1205:00 UT. At this time, corona aurora is observed at Upernavik. The peak electron energy corresponding to this aurora is about 300 eV with a number flux of  $>10^8$  els/cm<sup>2</sup>·sr·s.

The ion precipitation data during this period is also shown in Fig. 8. It is found that the large number flux of ion ( $>10^7$  ions/cm<sup>2</sup>·sr·s) is observed during this quiet condition. The region of large ion number flux is located at the region of impulsive

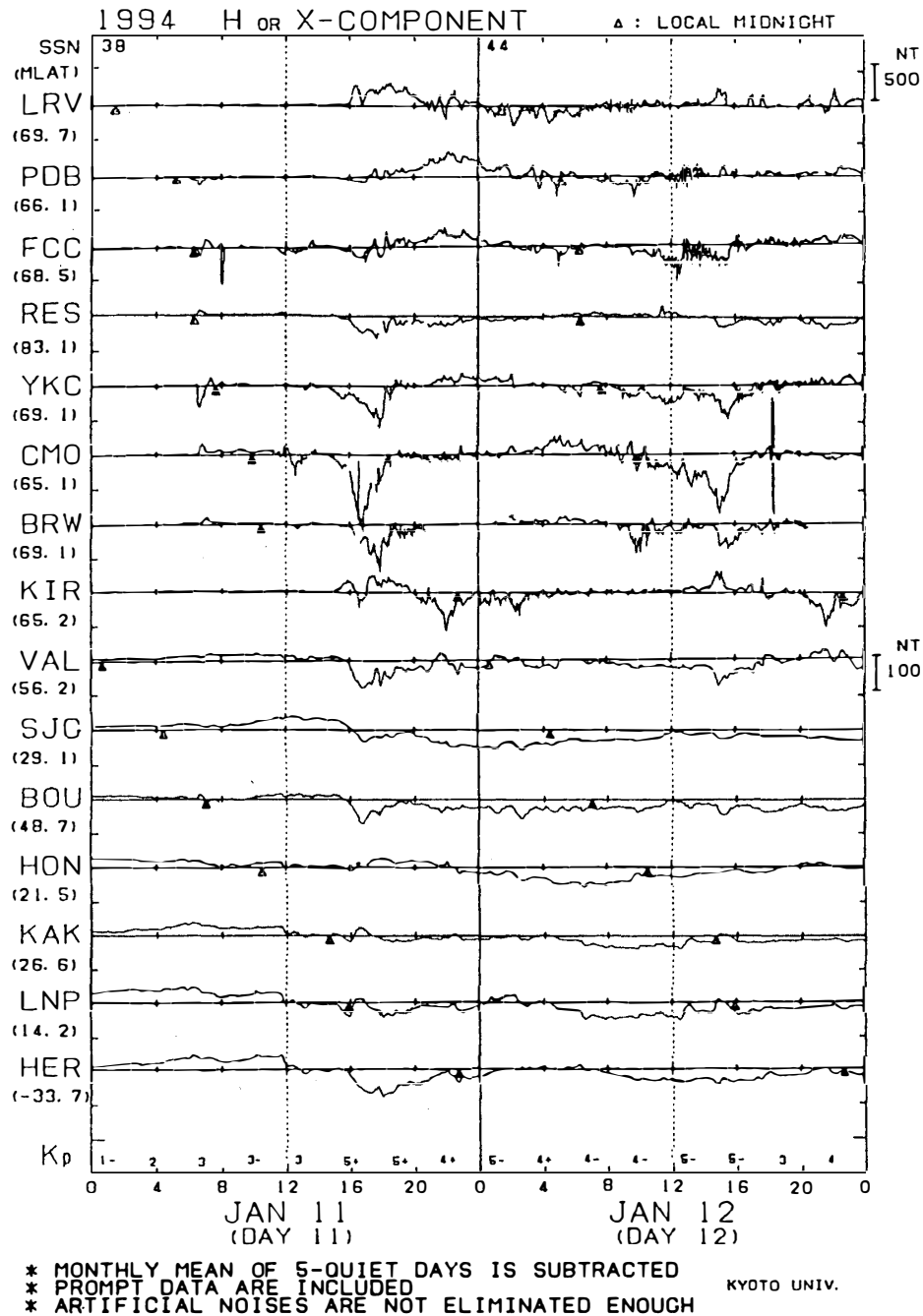


Fig. 9. The provisional geomagnetic data plots. The worldwide geomagnetic activity is high during the interval from 09h to 12h UT on January 12. Kp index in this period is 4-.

electron precipitation region. According to the ion data corresponding to corona aurora at Upernavik from 1203 to 1205 UT, ion precipitation with an energy of  $\sim 1$  keV and a number flux of  $\sim 10^7$  ions/cm<sup>2</sup>·sr·s is detected.

### 3. Dayside Aurora and Simultaneous Particle Precipitation during Disturbed Period

The auroral phenomena during disturbed period (09–12h UT, January 12, 1994) are

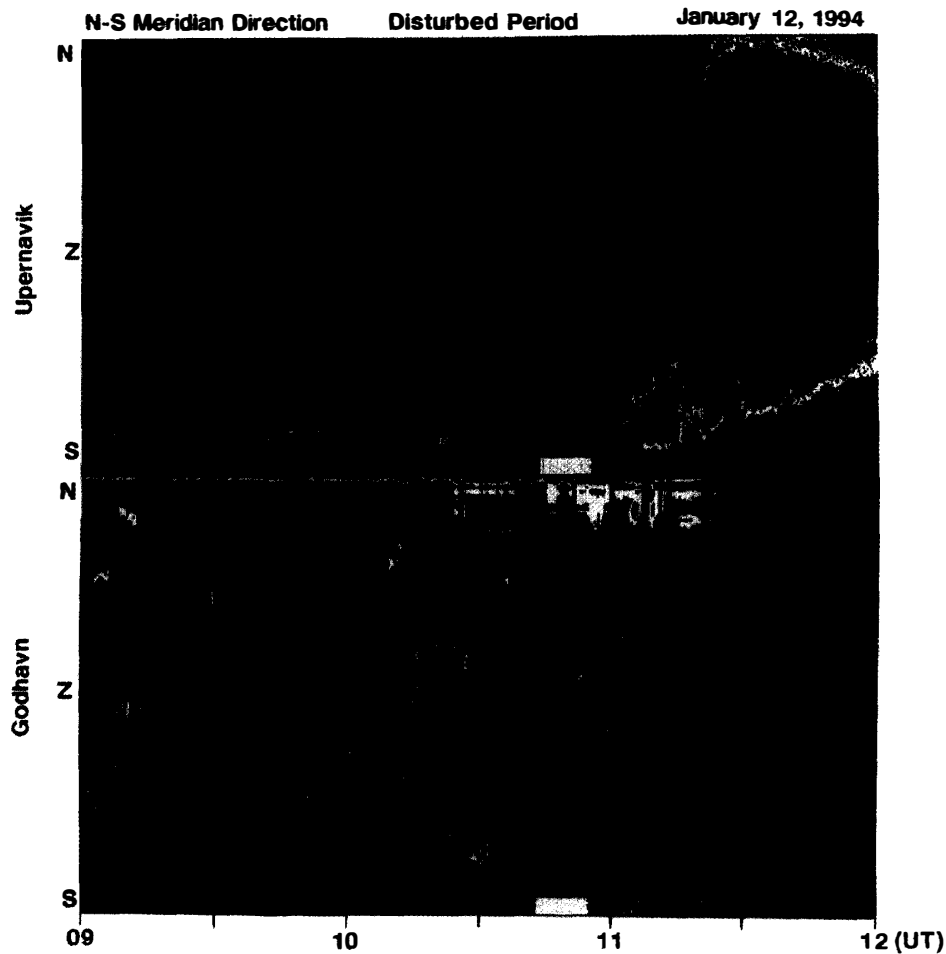


Fig. 10. The auroral dynamic spectra along the north-south meridian during the disturbed conditions. Upper and lower panels illustrate auroral spectra at Upernavik and Godhavn, respectively. Band auroras are seen near the equatorward horizon of Upernavik and bright auroras are observed near the zenith of Godhavn.

also examined by using Greenland and Spitzbergen auroral TV data. Figure 9 illustrates the provisional geomagnetic data plots (Kyoto University, 1994) during this period. The magnetic field at the high and low latitude regions is disturbed in this interval. The  $Kp$  index is continuously high with values of 4+ to 5. Unfortunately, IMF data is not available in this period.

The auroral dynamic spectra at two stations in Greenland are shown in Fig. 10. In the top panel, the dynamic spectra along the north-south meridian is obtained from all-sky TV data at Upernavik. The auroral activity is not so intense during the period from 09h to 11h UT. At this time, band auroras are observed above the equatorward horizon of Upernavik. The auroral activity becomes intense and the bright corona aurora moves poleward after 11h UT.

On the other hand, bright aurora appears at Godhavn during the period from 09 to 10h UT in the bottom panel. Discrete auroras propagate from the nightside region during this time. After 10h UT, corona auroras appear near the zenith and they shift to the poleward side. The center of auroral activity seems to be located near Godhavn during this disturbed condition. It is noted that quasi-periodic poleward motion is also

### Disturbed Period (January 12, 1994)

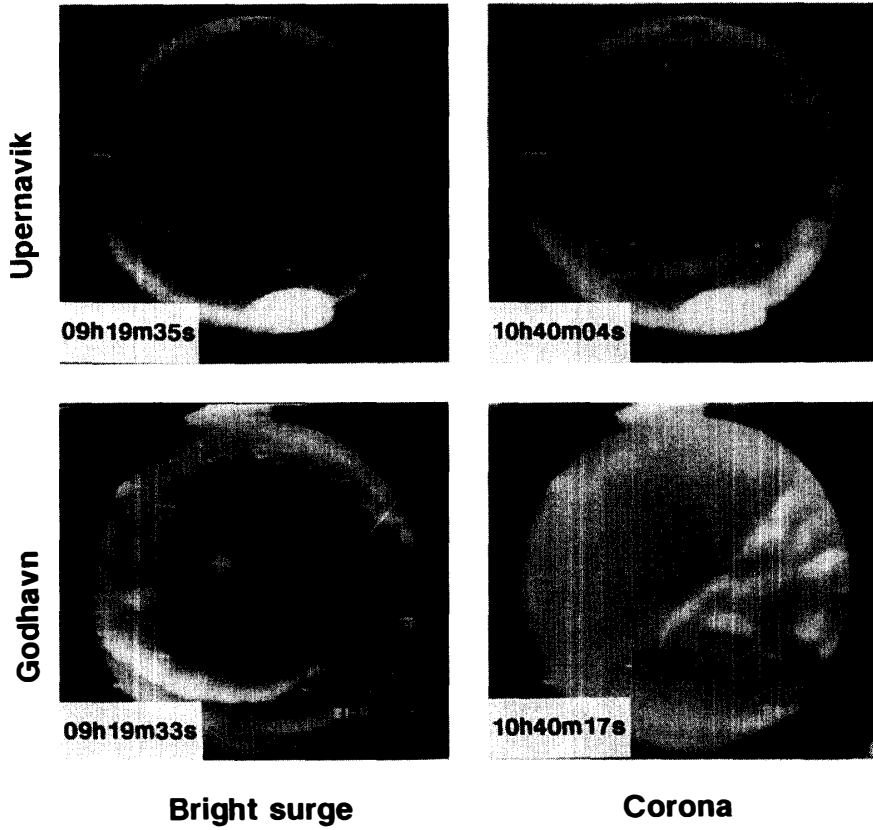


Fig. 11. All-sky TV camera data obtained at Upernavik and Godhavn. In the upper left and right panels (0919:35 and 1040:04 UT), band auroras are seen on the equator side of Upernavik. On the other hand, bright band and corona auroras are observed near the zenith of Godhavn as shown in the lower left and right panels (0919:33 and 1040:17 UT).

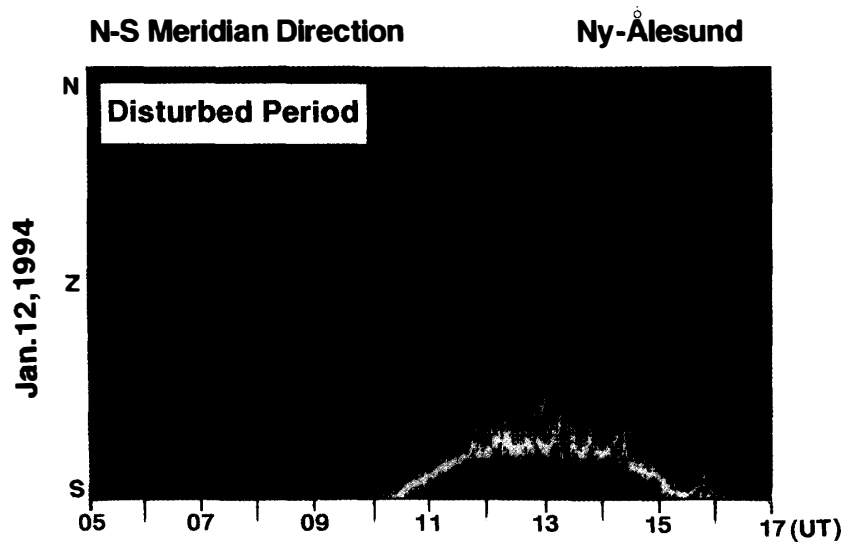


Fig. 12. The auroral dynamic spectrum obtained at Ny-Ålesund during the disturbed condition from 05 to 17h UT on January 12, 1994. Auroral activity was high during this interval.

recognized with its periodicity of about 300–400 s in this case.

Figure 11 shows all-sky TV data obtained at Godhavn and Upernavik. Upper and lower all-sky data are obtained at Upernavik and Godhavn, respectively. In the upper left data at 0919:35 UT, band auroras are seen on the equatorward side of Upernavik. These band auroras develop from the westward (the night side) and are continuously observed till 11 h UT. In the lower left data at 0919:33 UT, bright band appears on the equatorward side of Godhavn and develops from the nightside. In the upper right data at 1040:04 UT, band aurora is seen on the equatorward side of Upernavik and corona aurora is observed near the zenith of Godhavn as shown in the lower right panel. It is noted that the location of corona aurora shifts equatorward during the disturbed period.

Figure 12 shows the auroral dynamic spectrum obtained at Ny-Ålesund during the disturbed period from 05 to 17h UT on January 12, 1994. Discrete arcs are seen near the zenith during 05 to 07h UT and after then, corona auroras appear near the equatorward edge and move to the zenith. In the noon and post-noon sectors (09–14h UT), band-like auroras are observed near the zenith and move to the poleward side quasi-periodically. These band auroras also shifting from the evening to the noon side. The auroral data obtained at Ny-Ålesund indicates that the center of auroral activity is

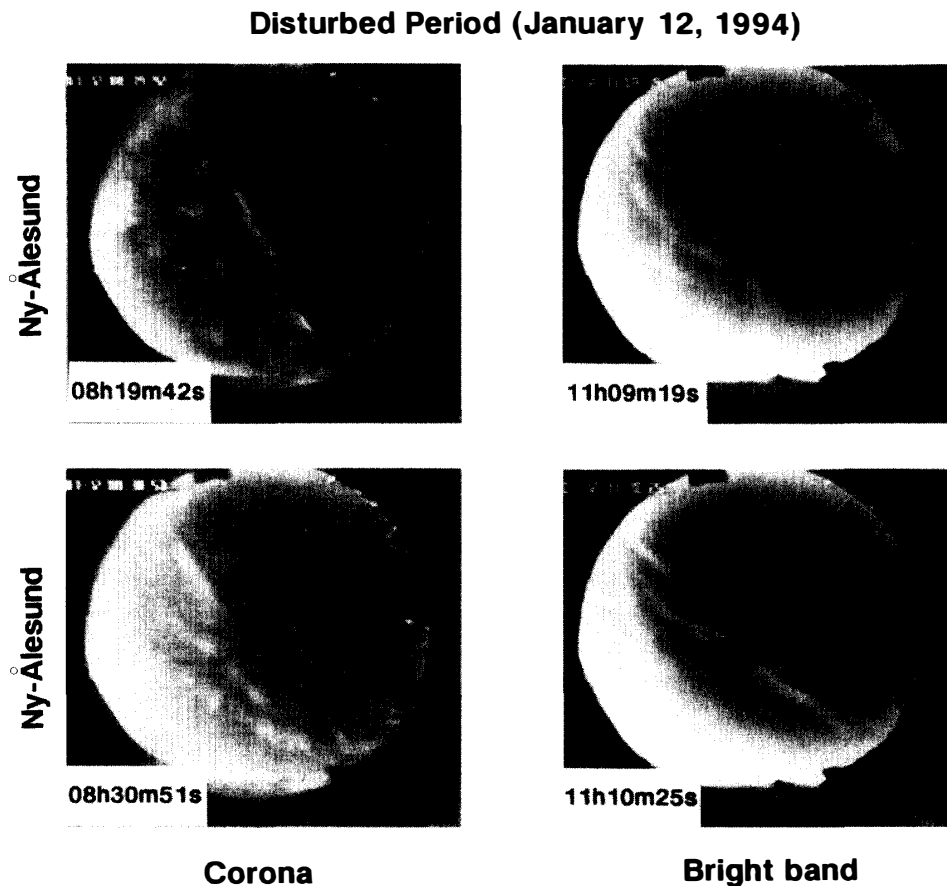


Fig. 13. All-sky TV camera data obtained at Ny-Ålesund. In the upper and lower left panels (0819:42 and 0830:51 UT), corona auroras are seen near the zenith of the station. On the other hand, band auroras developed from the night side as shown in the upper and lower right panels (1109:19 and 1110:25 UT).

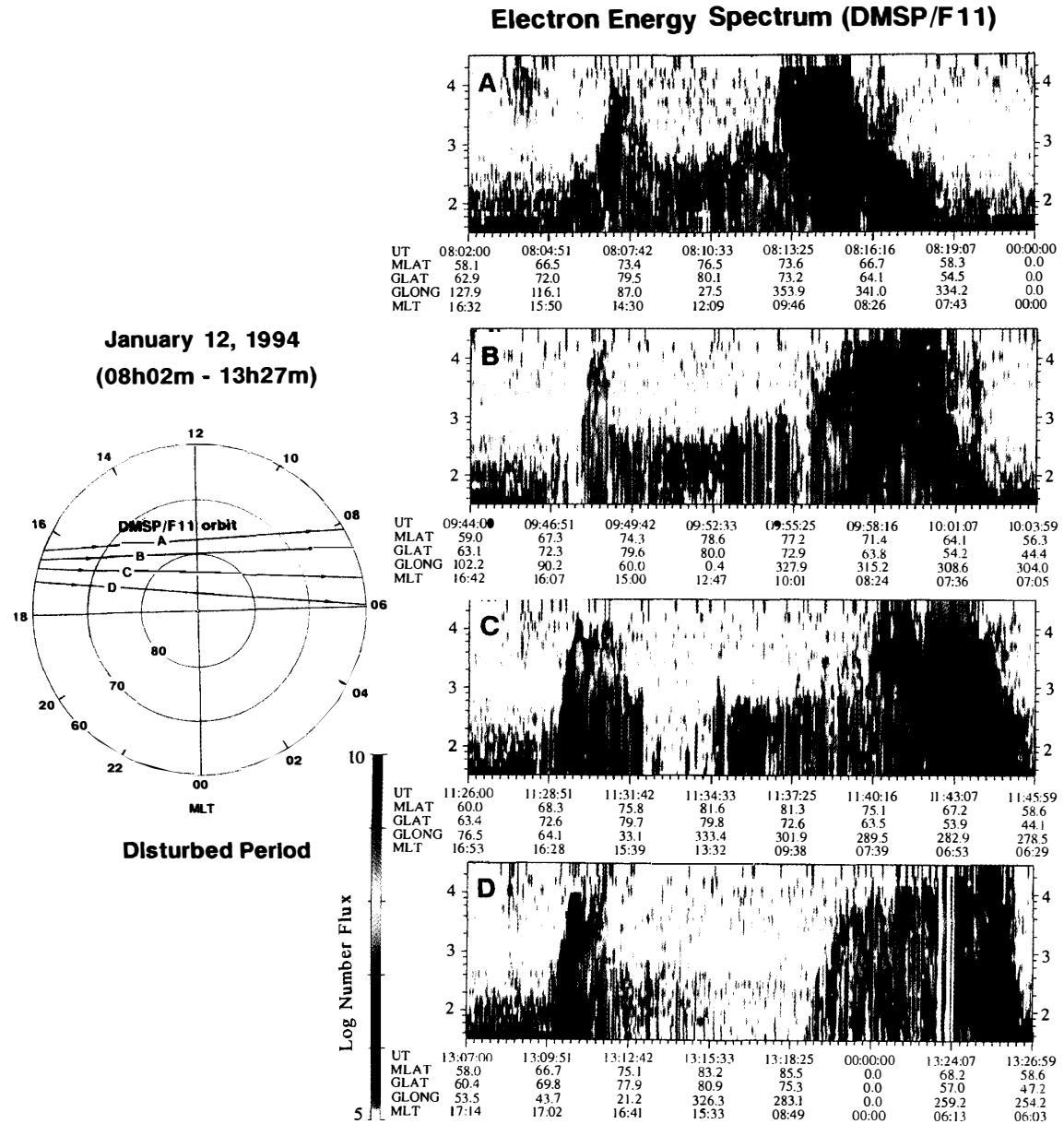


Fig. 14. DMSP/F11 satellite orbit and electron precipitation data during the disturbed condition from 0802 to 1327 UT. The right panel electron data (A, B, C, D) are obtained along A, B, C, D satellite orbit in the left panel. The polar cap boundary expands to the equator side in this period.

located near this station.

All-sky TV data at Ny-Ålesund are illustrated in Fig. 13. In the upper and lower left panel data at 0819:42 and 0830:51, corona auroras are recognized near the zenith. These corona auroras are similar to those observed at Godhavn as shown in Fig. 11. It is suggested that corona auroras exist continuously in the pre-noon sector during the disturbed period. From the upper and lower right panel data, band auroras are recognized at 1109:19 and 1110:25. These band auroras develop from the nightside and propagate to the dayside direction. In the post-noon sector, band auroras appeared instead of corona auroras.

Simultaneous particle data obtained by the DMSP F11 satellite are also examined for the disturbed period. Figure 14 illustrates electron precipitation data on January 12, 1994. The right panel electron data (A, B, C, D) correspond to the left panel orbits (A, B, D). The electron data A was obtained during the interval from 0802 to 0819 UT. Along this orbit, typical CPS electron precipitation is seen in the morning sector (0813–0818 UT) and high energy electrons ( $>1$  keV) BPS are seen in the evening sector ( $\sim 0806$  UT). The impulsive low energy electrons ( $<1$  keV) are seen near the noon sector. The electron data B was obtained during the period from 0944 to 1003 UT. The CPS precipitation is seen in the morning sector (0957–1000 UT) and high energy

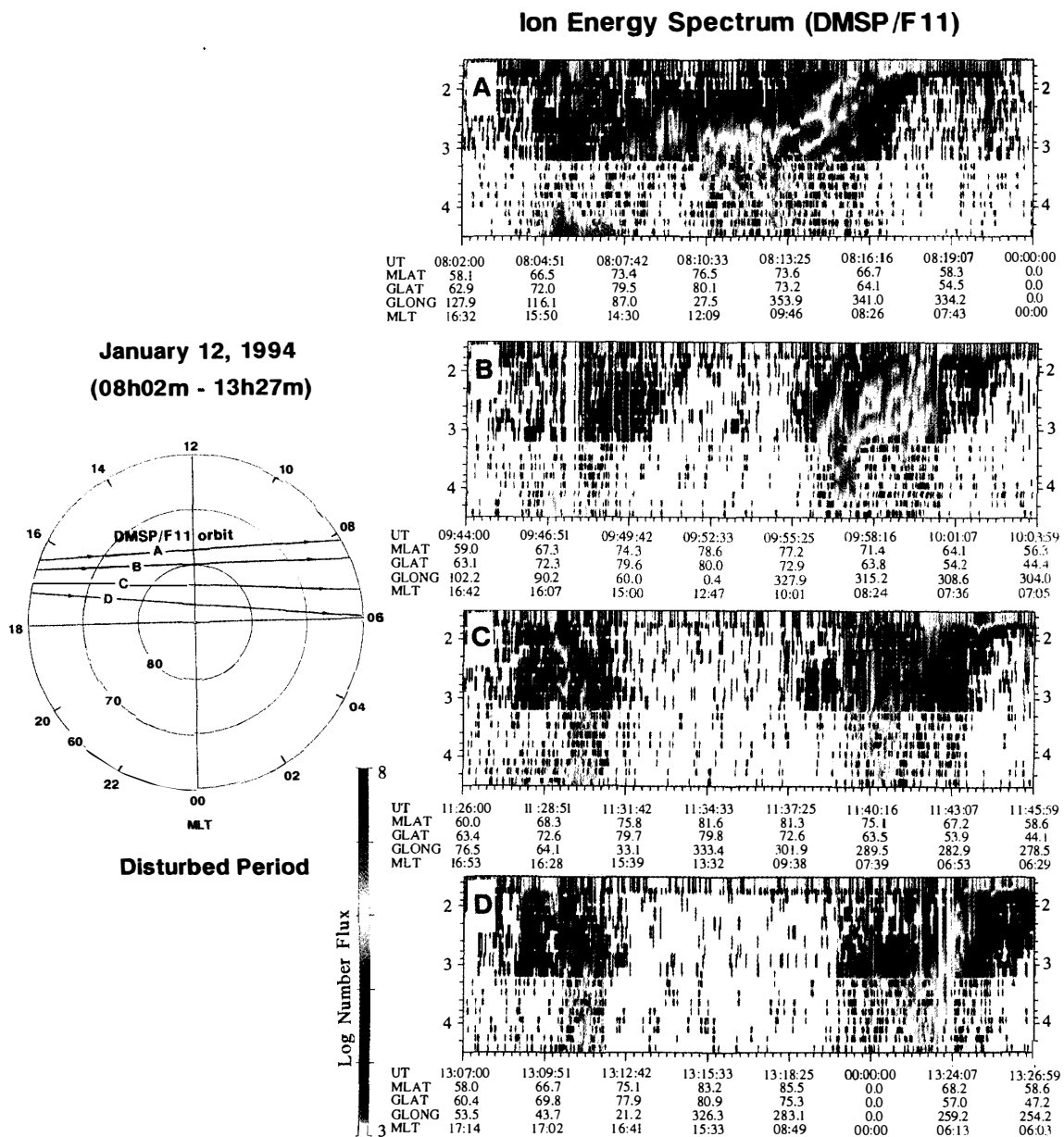


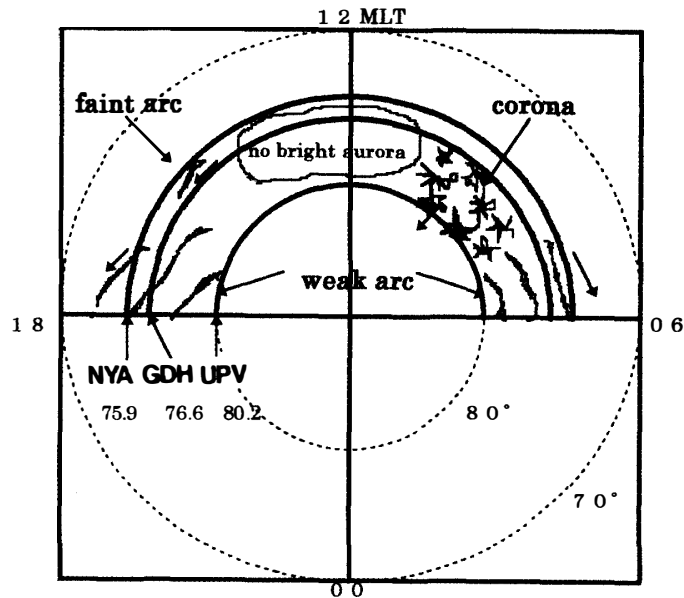
Fig. 15. DMSP/F11 satellite orbit and ion precipitation data during the disturbed condition from 0802 to 1327 UT. The right panel electron data (A, B, C, D) are obtained along A, B, C, D satellite orbit in the left panel. Ion precipitation regions in the dawn and dusk sectors shift to the equator side in this period.

electrons are also seen in the evening sector (0948 UT). Near the noon sector, impulsive low energy electrons are seen from  $75^\circ$  to  $80^\circ$  MLAT. The impulsive low energy electrons mostly embedded the high latitude region along A and B orbits. The electron data C was obtained during the period from 1126 to 1145 UT. The CPS precipitation is seen in the morning sector (1140–1145 UT) and high energy electron precipitation is seen in the evening sector (1129–1131 UT). The impulsive low energy electrons precipitate near the magnetic pre-noon sector and no significant precipitation is seen in the post-noon sector. The electron data D was obtained during the interval from 1307 to 1326 UT. The high energy precipitation including CPS is seen in the morning sector (1319–1326 UT) and high energy electron is also seen in the evening sector (1310–1312 UT). The impulsive electron precipitation is not clearly observed in the pre-noon sector in this orbit and the polar cap region expands equatorward during this disturbed condition.

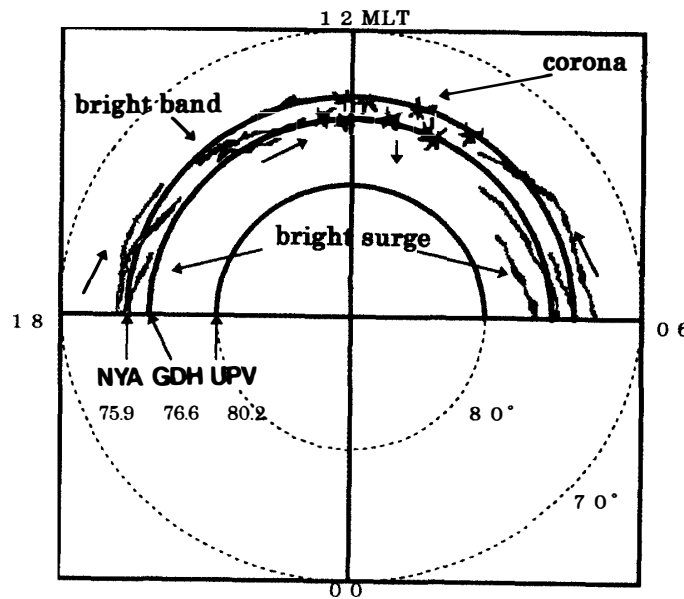
The ion precipitation during this period is also shown in Fig. 15. The region of intense ion precipitation corresponds to that of impulsive electron precipitation region. The region of dispersive ion precipitation corresponds to the CPS region respectively. It is noted that the ion precipitating regions in the dawn and dusk sectors shift equatorward. Their number flux ( $\sim 10^6$  ions/cm<sup>2</sup>·sr·s) is not so large as compared to that observed during quiet period. The empty region of ion precipitation is recognized near the magnetic pole in orbits B, C, and D. Generally, the size of the empty region of ions in Fig. 15 is larger than that of electrons in Fig. 14. In this period, there are no satellite orbit which pass over the region of all-sky TV image coverage at Ny-Ålesund. Generally, the electron energy corresponding to impulsive electron precipitation during disturbed period ( $>1$  keV) becomes higher than that during quiet period ( $<500$  eV). Therefore, we consider that the electron energy of corona aurora increases during disturbed period.

#### 4. Summary and Discussion

From the auroral observations at Greenland and Spitzbergen, the characteristics of quiet and disturbed dayside aurora are examined and results are summarized in Fig. 16. It is a remarkable point in this paper to show the general characteristics of dayside auroras. Namely, corona auroras are seen in the pre-noon sector and band auroras are seen in the post-noon sectors. It is noted that we combined other day's auroral event and also used other observatory's data (S. Stromfjord, South Pole, Zhongshan St.) in order to illustrate Fig. 16. The upper panel of this figure illustrates the dayside auroral pattern during quiet period. The weak arc aurora from the dayside region is observed in the dawn and dusk sectors. This is traditionally called sun-aligned arc (LASSEN and DANIELSEN, 1978). The appearance of this weak arc is usually observed at the latitude of  $75^\circ$  or less MLAT during northward IMF conditions. From auroral observation at Godhavn and S. Stromfjord ( $74.0^\circ$  MLAT) in Greenland, weak arc is frequently observed in the dusk sector during the quiet period (typical images are not shown in this paper). In the pre-noon sector, corona aurora with ray structure appears at  $75^\circ$ – $80^\circ$  MLAT. This corona aurora moves poleward quasi-periodically. The occurrence periodicity of this corona is about 300–400 s in this case. Near the noon sector, the



Quiet Period (Jan. 10, '94)



Disturbed Period (Jan. 12, '94)

Fig. 16. Upper and lower panels illustrate dayside aurora patterns during quiet and disturbed period.

bright aurora is not observed at Ny-Ålesund ( $75.9^\circ$  MLAT). It is uncertain whether the bright aurora exists at the higher latitude side of Ny-Ålesund by using one point observation. From the examination of particle data by DMSP satellite, significant particle precipitation is observed at the higher latitude side of Ny-Ålesund. Therefore, the faint aurora may be existing at latitudes higher than  $80^\circ$  during this quiet period. In the post-noon sector, faint arc appears near the zenith of Ny-Ålesund. This arc is very faint and its appearing period is about 10 min. The movement direction of this faint arc

is from the dayside to the evening side.

The lower panel of Fig. 16 shows the dayside auroral pattern during the disturbed period. Bright surge auroras are observed in the dawn and the dusk sector (typical images are not shown in this paper). These surges seem to propagate from the night side during the recovery phase of substorm. The appearing region of the surge auroras are at about  $75^\circ$  MLAT or less. Near the noon sector, active corona auroras appear at the latitude lower than  $75^\circ$  MLAT. These corona auroras periodically move poleward with the period of 300–400 s. The appearing region of the corona auroras during the disturbed period is located at the latitude lower than that during the quiet period by about  $3^\circ$ .

In the post-noon sector, bright band aurora appears during the disturbed period. The bright band aurora shows periodic poleward movement with a period of 100–150 s. These periodic movements may be related to the compressional Alfvén waves near the magnetopause as suggested by ELPHENSTON *et al.* (1993). There is a discontinuity of auroral intensity between bright band in the post-noon sector and bright surges in the dusk sector. Therefore, the sources of bright band and bright surges seem to be different.

From the examination of dayside auroral data under the quiet and disturbed conditions, characteristics of auroral patterns are quite different in the pre-noon and post-noon auroras for the different magnetic activities. In the pre-noon sector, weak arc is observed in the dawn and dusk sectors and corona auroras appear in the pre-noon sector during quiet period. AYUKAWA *et al.* (1996) compared electron precipitation data between corona and weak arc phenomena. They show that the peak electron energy of corona aurora is a few hundred eV and that of weak arc is about 100 eV. From the DMSP satellite data reported by Newell *et al.* (1991), plasma mantle electrons (energy is  $\sim 100$  eV) are energy of lower than those at low latitude boundary layer (LLBL, a few hundred eV). Therefore, we consider that the source of weak arc is plasma mantle and corona aurora is originated in LLBL. There are no bright auroras near the noon and post-noon sector during quiet period. From the particle observations by DMSP satellite, significant precipitation (100 eV  $\sim$  a few hundred eV) is recognized on the higher latitude side of the ground observatory. So these higher latitude electrons seem to be also originated in LLBL and partly in plasma mantle.

On the other hand, during the disturbed period, bright surge auroras propagating from the night side are observed in the dawn and dusk sectors. These auroras are very bright and originated from the boundary plasmasheet. Near the pre-noon sector, active corona auroras are frequently observed and the region of these coronas is at latitudes lower than  $77^\circ$  MLAT. The corona region in this period is by  $3^\circ$  lower than that during the quiet period. Since the location of LLBL shifts equatorward as the magnetic activity increases, these corona auroras seem to be related to LLBL. In the post-noon sector, bright band auroras appear and these auroras periodically appear one by one. It is not clear what condition determines this periodicity. The magnetic local time of this aurora corresponds to the upward field aligned current region. So we consider that compressional Alfvén wave excited near post-noon magnetopause (LLBL) due to the solar wind fluctuations (*e.g.*, impulse of density or interplanetary magnetic field variations) propagates to the inner magnetosphere and induce the particle acceleration along the field line.

Although the periodicity is different between bright band (100–150 s) and corona aurora (300–400 s), a similar process may occur for corona auroras.

In this paper, we showed the morphology of dayside aurora obtained at ground-based observations. Generally, multi-points ground observation will give us the temporal and spatial auroral variations which are difficult to obtain from satellite data. Therefore, it must give us some essential information of the solar wind and magnetosphere interaction process. It is also useful to make clear how these variations relate to substorm development. We plan to compare these dayside auroral events with particle and field data obtained with low- and high-altitude satellites.

#### References

- AYUKAWA, M., MAKITA, K., YAMAGISHI, H., EJIRI, M. and SAKANOI, T. (1996): Characteristics of polar cap aurora. *J. Atmos. Terr. Phys.*, **58**, 1885–1894.
- AYUKAWA, M., MAKITA, K., NISHINO, M. and YAMAGISHI, H. (1997): Comparison between prenoon and postnoon auroras during quiet and disturbed conditions I (extended abstract). *Proc. NIPR Symp. Upper Atmos. Phys.*, **10**, 142–146.
- EGELAND, A., CARLSON, H.C., DENING, W. F., FUKUI, K. and WEBER, E. (1992): Day-side auroral signatures based on simultaneous coordinated observations at Svalbard and Greenland. *IEEE Trans. Plasma Sci.*, **20**, 726–739.
- ELPHINSTONE, R. D., MURPHREE, J. S., HEARN, D. J., COGGER, L. L., NEWELL, P. T. and VO, H.B. (1992): Observations of the UV dayside aurora and their relationship to DMS particle boundary definitions. *Ann. Geophys.*, **19**, 815–826.
- ELPHINSTONE, R. D., HEARN, D. J., MURPHREE, J. S., COGGER, L. L., JOHNSON, M. L. and VO, H. B. (1993): Some UV dayside auroral morphologies. *Auroral Plasma Dynamics*, ed. by R. L. LYSAK. Washington, D.C., Am. Geophys. Union., 31–45 (Geophys. Monogr. 80).
- FASEL, G. J., MINOW, J. I., LEE, L. C., SMITH, R. W. and DEEHR, C. S. (1994): Poleward-moving auroral forms: What do we really know about them? *Physical Signature of Magnetospheric Boundary Layer Process*, ed. by J. A. HOLTET and A. EGELAND. Dordrecht, Kluwer Academic, 211–226.
- Kyoto Univ. (1994): Provisional geomagnetic data plots. *Data Anal. Cent. Geomag. Space Mag. Fac. Sci.*, **10**, 7–8.
- LASSEN, K. and DANIELSON, C. (1978): Quiet time pattern of auroral arcs for different directions of the interplanetary magnetic field in the Y-Z plane. *J. Geophys. Res.*, **83**, 5777–5789.
- MENG, C.-I. (1994): Space borne optical remote sensing of midday auroral oval and different participation regions. *Physical Signature of Magnetospheric Boundary Layer Process*, ed. by J. A. HOLTET and A. EGELAND. Dordrecht, Kluwer Academic, 211–226.
- NEWELL, P. T., BURKE, W. J., SANCHEZ, E. R., MENG, C.-I., GREENSPAN, M. E. and CLAUER, R. (1991): The low-latitude boundary layer and the boundary plasma sheet at low altitude: Prenoon precipitation regions and convection reversal boundaries. *J. Geophys. Res.*, **96**, 21013–21021.
- SANDHOLT, P. E., LYBEKK, B., EGELAND, A., NAKAMURA, R. and OGUTI, T. (1989): Midday auroral breakup. *J. Geomagn. Geoelectr.*, **41**, 371–387.
- SANDHOLT, P. E., EGELAND, A., LYBEKK, B., DEEHR, C. S., SIVJEE, G. G. and ROMICK, G. J. (1983): Effects of interplanetary magnetic field and magnetospheric substorm variations on the dayside aurora. *Planet. Space Sci.*, **31**, 1345–1362.
- SMITH, R. W. (1994): Dayside aurora and magnetopause processes. *Physical Signature of Magnetospheric Boundary Layer Process*, ed. by J. A. HOLTET and A. EGELAND. Dordrecht, Kluwer Academic, 211–226.
- SOUTHWOOD, D. (1987): The ionospheric signature of flux transfer events. *J. Geophys. Res.*, **92**, 3207–3213.
- VOROBYEV, V. G., GUSTAFSSON, G., STARKOV, G. V., FELDSTEIN, Y. I. and SHEVNINA, F. (1975): Dynamics of day and night aurora during substorms. *Planet Space Sci.*, **23**, 269–278.

*(Received December 9, 1997; Revised manuscript accepted May 7, 1998)*